JOURNAL OF MATERIALS SCIENCE 37 (2002) 2801 – 2810

Comparison of the deformation and failure characteristics of morphologically distinct metal-glass interpenetrating phase composites

J. J. HARRIS, P. M. MARQUIS
The University of Birmingham, Biomaterials, The School of Dentistry, St Chad's Queensway, Birmingham B4 6NN, UK

Deformation and failure characteristics of two metal-glass interpenetrating phase composite (IPC) systems were compared against a single-phase glass control. The first system (Captek-P) comprised an interleaved arrangement of flake-shaped Au/Pt/Pd particles, the second (Captek-G) comprised loosely packed spherical Au particles. Both materials contained a fully interconnected network of porosity, formed by thermal fusion of particles at contact points. Glass was infiltrated into the porous networks by capillary action at high temperature. Mechanical properties were evaluated using three-point bend tests and compared to data from the glass control. The strength of the glass control (123.47 MPa) was not significantly different to that of either IPC, however both Captek-P and Captek-G IPCs displayed significantly reduced elastic moduli (55.2 ± 10.6 GPa and 48.4 ± 12.4 GPa respectively) compared with the glass (91.5 ± 9.6 GPa). In addition to significantly higher relative toughness than the glass control the IPC materials exhibit plastic deformation prior to failure. Mixed fracture modes were evident on fracture surfaces. Corresponding stress-strain profiles for the materials show well-defined linear elastic regions that make a gradual transition into plastic behaviour. Strength of the glass control decreased by 28% upon exposure to moisture, a feature echoed by the Captek-G IPC system, however not by the Captek-P IPC, indicating that the morphology of the interpenetrating reinforcement can significantly affect the mechanical properties of IPCs.

1. Introduction

Multi-phase materials in which constituent phases are mutually continuous and interconnected in three dimensions can be termed interpenetrating phase composites (IPCs). A wide range of methods for IPC manufacture exists. Capillary infiltration of low viscosity material into a network of porosity has been achieved passively [1, 2], and with pressure assistance [3]. *In situ* reaction-based methods of manufacture include reactive metal penetration by sacrificial oxide displacement [4, 5], self-propagating high-temperature synthesis (SHS) reactions [6, 7] and reactive hot isostatic pressing (HIPing) [8, 9]. Other techniques include spinodal decomposition of phase-separated glass systems [10] and a rapid prototyping method known as three-dimensional printing [11].

The principal novelty of IPCs lies in their potential to allow tailoring of mechanical properties through combination of dissimilar materials. Recent finite element modelling (FEM) studies suggest that the most dramatic property gains are only realized when the properties of the constituent phases are considerably different [12], since the theoretical upper and lower bounds on bulk properties are widely separated. The authors of this particular study further state that where component properties are broadly similar volume fraction has a greater effect on final IPC properties than microstructural differences. However mechanical properties such as strength and toughness are not the sole beneficiaries of the IPC configuration. In the late 1970s piezoelectric IPCs, manufactured by a replamineform process using natural coral as the original template, were produced. The replamineform composites yielded favourable properties in comparison to homogenous materials and it was suggested [13] that, in conjunction with their reduced density, such materials should make strong candidates for passive device applications such as marine hydrophones. More recently IPC materials with strengths of approximately 0.5 GPa, good electrical conductivity and low density have been offered as attractive propositions for heat sink materials or lightweight structural parts [14].

However the dominant focus on IPCs over the last decade has been on the strength, toughness and elastic property modifications which can be achieved when ceramic preforms of varying porosities are infiltrated with a metallic phase. It has been shown in a Ni_3Al/Al_2O_3 IPC system that the strength at 800°C is comparable with that achieved at room temperature [15] suggesting suitability for high temperature structural applications. The range of potentially attractive properties that can result from the tri-dimensional interpenetration of

two dissimilar materials is therefore broad, but despite this few systems have reached the stage of commercial implementation. Two notable exceptions that are already commercially available were developed with dental restoration in mind. The challenge in producing dental crowns is to deliver a combination of accuracy of fit to the prepared tooth combined with translucency and a variety of shade to match the natural dentition. In addition the materials must be capable of delivering a capacity to be manufactured individually to match the needs of a single patient at a low economic cost. Materials used in such systems must also have sufficient strength and rigidity to provide resistance to masticatory forces in the constantly moist oral environment. The two existing IPC crown systems are Captek (Davis Schottlander and Davis Ltd, Herts, UK), a metal-metal IPC system for the fabrication of high gold copings for porcelain-fused-to-metal (PFM) crowns and In-Ceram (Vita, Bad Säckingen, Germany), an alumina-glass IPC used in the manufacture of all ceramic dental crowns. Captek is marketed as an alternative to conventional casting methods of coping manufacture for dental crowns and is claimed to be an attractive option given that the processing route (infiltration of a low viscosity second phase into a porous preform) results in minimal firing shrinkage and hence accurate marginal regions of dental restorations. The principal feature of In-Ceram, aside from its aesthetic acceptability, is its high strength reported to exceed 500 MPa in three-point bend [16–18]. The significance of these materials to this manuscript lies in the fact that they provide the basis of the brittle-ductile systems we shall describe.

Captek is supplied as two components "P" and "G", each in the form of a ribbon comprising a dispersion of metal particles in an organic binder. The P material, (Au/Pt/Pd) when fired according to manufacturers instructions, becomes a preform containing a highly convoluted network of porosity, as shown in Fig. 1. This network formation arises from the volatilisation of the organic binder from the interleaved arrangement of metal particles in the as-supplied ribbon, which subsequently fuse at points of contact to provide intrinsic mechanical stability. Conventionally the G material (spherical particles of Au) would be burnished (in its as-supplied condition) over the fired P preform and a further thermal cycle carried out to eliminate the organic content and cause the gold to melt and infiltrate the porous pre-form by capillary action.

A finished In-Ceram component results from the infiltration of a porous alumina preform with a lanthanum-aluminosilicate glass at high temperature. This glass was originally formulated to deliver a low viscosity and a high refractive index to match that of the alumina reinforcement to optimise aesthetics. The resulting wetting characteristics of this glass render it capable of infiltrating sub-micron pores in the In-Ceram alumina preform and it has been shown that the glass can be sintered to near full density from the powder condition in approximately one minute at 840°C [19].

A series of trial experiments revealed that carefully controlled thermal treatment of the Captek-G material would result in the production of a porous preform having a significantly different network morphology (as demonstrated in Fig. 2) to the P material, arising from point fusion of near-spherical particles. This, in combination with the potentially favourable sintering/infiltration characteristics of the In-Ceram glass and

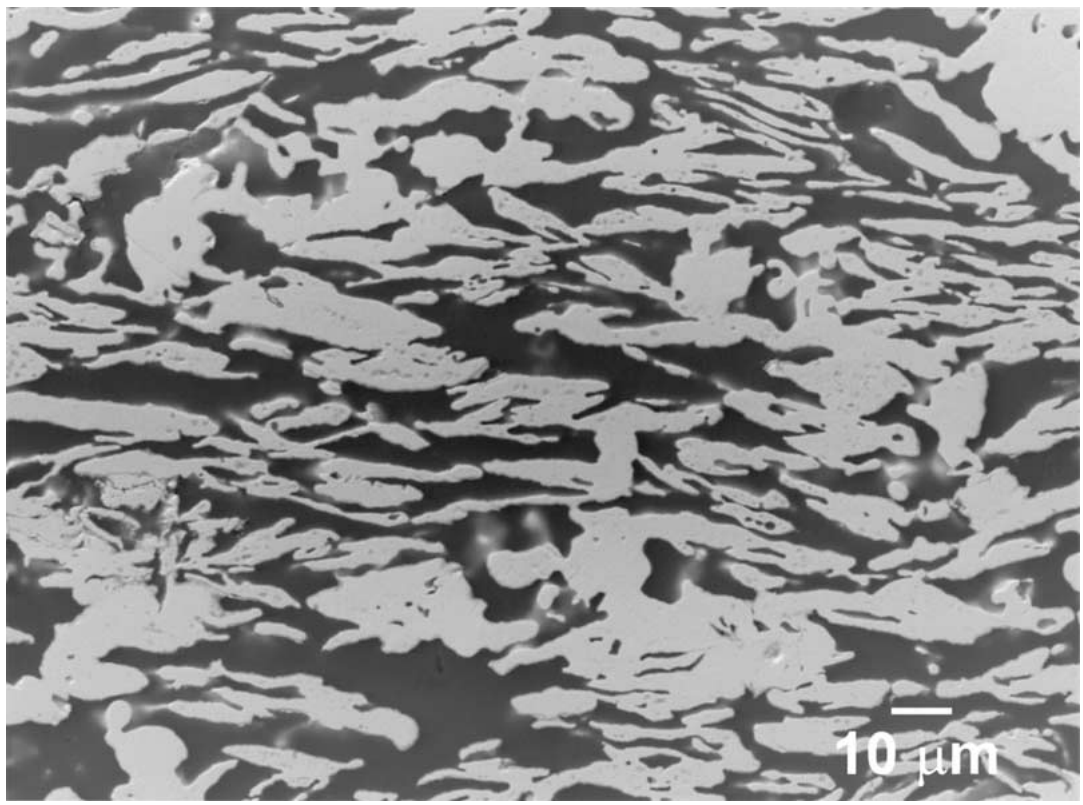

Figure 1 Backscattered SEM micrograph at ×750 magnification of a longitudinal cross section through a Cap-P preform after thermal dewaxing at 1,075°C for 4 mins.

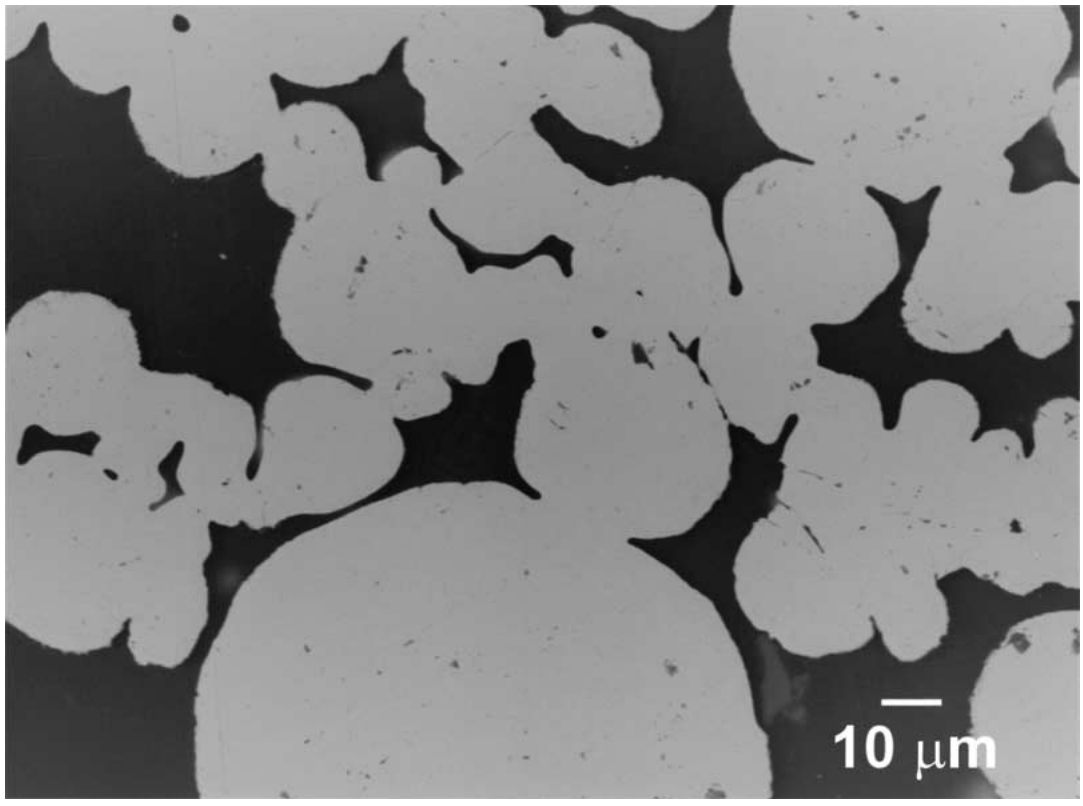

Figure 2 Backscattered SEM micrograph at ×750 magnification of a longitudinal cross section through a Cap-G preform after thermal dewaxing at 1,025°C for 4 mins.

the fact that all materials were commercially available, requiring no development of their own, suggested that a novel production route for IPCs (infiltrating glass into metal) would be worthy of further investigation. Of particular interest was the potential simplicity of the production route by which two separate IPCs of differing morphology could be constructed. In this manuscript we describe the manufacture of such brittle-ductile IPC systems and explore their mechanical properties in terms of strength, elastic modulus, and relative toughness. The effect of a moist storage and testing environment on these parameters is also described.

2. Experimental procedure

Captek-P (Cap-P) and Captek-G (Cap-G) materials, supplied in strip form, were sliced using a razor blade to create bars approximately 3 mm × 23 mm × 0.22 mm and placed on blocks (12 mm × 30 mm × 4 mm) of the manufacturers refractory die material (Capvest - Davis Schottlander & Davis, Herts, UK). Thermal treatment for the Cap-P material was carried out according to the manufacturer's recommendations, however the Cap-G material was fired according to the most suitable firing schedule discovered during the trial experiments. Firing treatments for both components are summarised in Table I and were performed using a Biodent Mulitmat furnace (DeTrey, London, UK) to remove the organic binder and cause interparticle fusion to create the porous network. This process is referred to as "dewaxing". Glass infiltration was carried out by applying a thin slurry of In-Ceram glass powder (Vita Shade A3.5, Vita, Bad Säckingen, Germany) to the surface of the metallic preform that was uppermost during the dewaxing stage. Coated preforms were then inverted and placed onto a sheet of platinum foil and heat treated to allow the glass to infiltrate the interconnected porosity by capillary action. Infiltration firing cycles for the Cap-P and Cap-G materials were individually tailored owing to the difference in melting characteristics of each metallic phase as identified in the trial experiments described earlier. The Cap-P IPC was infiltrated with glass at 1,025°C for 2 hours. The reduced melting temperature and more open network of porosity within the Cap-G preform meant that 1,025°C for only 4 minutes was sufficient to infiltrate the glass without adversely affecting the metallic phase in the Cap-G IPC system. Following glass infiltration the excess glass at the surface of infiltrated bars was removed using a rotary handpiece fitted with a medium grit diamond burr (BGU247-Unodent, Markt Schwaben, Germany), followed by two successively less abrasive polishing stones (FL4 Dura-Green Stone & FL2 Dura-White Stone respectively-Shofu Dental Products Ltd, Kent, UK). Bars of In-Ceram glass (Vita Zahnfabrik, Vita Shade A3.5) approximately 2.7 mm wide and 0.3 mm thick were sectioned from a block using an Isomet Low Speed Saw (Beuhler, Illinois, USA) fitted with a 100 mm Diamond Cut-off Wheel (Struers, Glasgow, Scotland).

TABLE I Firing cycles employed for metallic preform manufacture

Material	Captek-P	Captek-G
Start temp (°C)	500	500
Heating rate (°C/min)	80	80
High temp (°C)	1,075	1,025
Hold time (min)	4	4

TABLE II Summary of all data obtained for each material tested

Material	Vol% pore/glass phase	Flexural strength (MPa)	Elastic modulus (GPa)	(Normalised) area under curve
In-Ceram glass (Dry)	100 ± 0	123.5 ± 15.4	91.6 ± 9.6	21.6 ± 5.1
In-Ceram glass (Wet)		89.0 ± 13.8	84.8 ± 15.2	11.6 ± 2.4
Cap-P IPC (Dry)	$29. \pm 2.8$	135.6 ± 29.7	55.2 ± 10.7	69.3 ± 28.2
Cap-P IPC (Wet)		146.3 ± 24.3	45.3 ± 11.6	100 ± 31.9
Cap-G IPC (Dry)	32.4 ± 6.4	124.2 ± 19.9	48.4 ± 12.5	66.9 ± 24.5
Cap-G IPC (Wet)		84.0 ± 16.9	49.9 ± 16.6	62.2 ± 23.2

The contact edge of the cut-off wheel was lubricated at all times during sectioning using DP-Lubricant Blue (Struers, Glasgow, Scotland). Specimens required for mechanical testing under ambient conditions were then stored, prior to use, in a dessicator at room temperature. Those to be tested wet were placed in distilled water and maintained at $37 \pm 1^{\circ}$C for a minimum of 120 hours before testing. For each group of samples the final number tested was 20 in each case. Samples stored in water at 37°C were allowed to passively return to room temperature in water prior to mechanical testing due to difficulties with maintaining an artificially raised temperature during the testing procedure.

Three-point bend apparatus comprised cylindrical supports (1 mm in diameter) with a support span of 15 mm. The load was applied centrally at 90° to the long axis of the specimen at a crosshead speed of 0.01 mm/min using an Instron 5544 load frame (Instron Ltd, Buckinghamshire, UK). This crosshead speed was chosen to allow the maximum amount of time for slow crack growth to take place within the specimen. Wet testing of specimens was carried out on identical apparatus submerged in distilled water at room temperature. Specimen strength was calculated according to Equation 1.

$$\sigma = \frac{3Pl}{2bd^2} \tag{1}$$

where σ represents flexure stress (MPa); P is the maximum load (N); l the support span (mm); b is the specimen width (mm) and d the specimen thickness (mm). Strain was calculated relative to crosshead extension according to Equation 2,

$$\varepsilon = \left(\frac{6Dd}{L^2}\right) \times 100 \tag{2}$$

where ε is strain (%); D is the mid-span deflection (mm); d the specimen thickness (mm) and L is the support span (mm). The linear elastic region of each specimen's stress-strain output was identified using a series of regression analyses applied from the beginning of the data set to a serially increased number of data points until $R^2 \leq 0.95$. At this point the plot was deemed to be moving away from linear behaviour and so only those points isolated by the penultimate regression analysis were included in calculation of elastic modulus, which was achieved using Equation 3,

$$E = \frac{L^3 m}{4bd^3} \tag{3}$$

where E represents the elastic modulus (MPa); L the support span (mm); b is the specimen width (mm), d the specimen thickness (mm) and m is the gradient of the linear elastic region of the stress-strain curve as identified by the equation of the linear trend-line through the points identified by the regression analysis. Specimen toughness was inferred by calculation of the area under the stress-strain curve to the point of final specimen failure.

Cross-sections were obtained from specimens embedded in Epofix cold-mounting resin (Struers, Glasgow, Scotland, UK). A planar surface was produced using a graded series of silicon carbide papers (varying from P200–P4,000), sequentially fitted to a Dap-7 Grinding and Polishing Wheel equipped with a Pedemin attachment (Struers, Glasgow, Scotland, UK). Specimens were treated at each grade of paper for 25 seconds, under an applied force of 25 N, with a continuous stream of water providing lubrication. Final polishing of planar surfaces was carried out using 3 μm and 1 μm polycrystalline diamond suspensions (Struers, Glasgow, Scotland, UK) applied to two separate DP-Dac polishing cloths (Struers, Glasgow, Scotland, UK) for 30 seconds and 1 minute respectively. All samples were gold coated for 40 seconds using a Desk II Sputter-Coater (Denton Vacuum, New Jersey, USA) to reduce the incidence of surface charging in the SEM.

Analysis of both sample microstructures and fracture surfaces was accomplished using Scanning Electron Microscopy (SEM) (Jeol JSM 5300 LV - Jeol Ltd, Akishima Tokyo, Japan). Secondary electron imaging was used to analyse the surface morphology of the samples under investigation, whilst backscattered electrons were employed to provide compositional information. Digitised SEM images of composite cross-sections, obtained using constant working distance, magnification and beam conditions, were analysed with Optimas 6.5 image analysis software (Media Cybernetics, MD, USA) in order to quantify the relative volume of constituent materials in the composite. For each sample group a total of 20 separate images were obtained, however to ensure that representative data was produced, specimens were sectioned at serially adjusted depths and a maximum of 2 images were obtained from one individual specimen.

3. Results

A full summary of the data produced for comparative purposes is shown in Table II. Three-point bend test data (summarised in Fig. 3) indicates that the strength

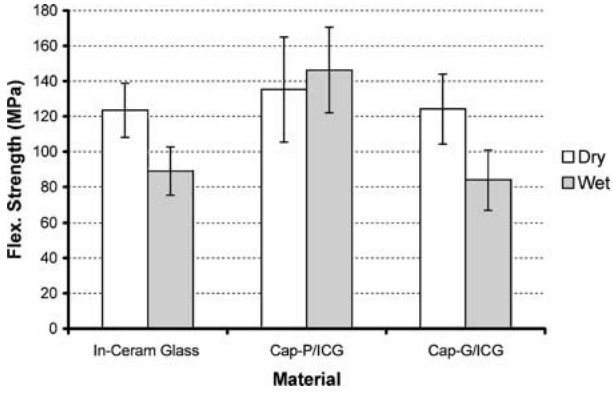

Figure 3 Histogram showing the mean flexural strength (MPa) calculated for each material in the study, tested both in air and in water. Vertical error bars show the standard deviation for each sample. The number of specimens (n) = 20 in all cases.

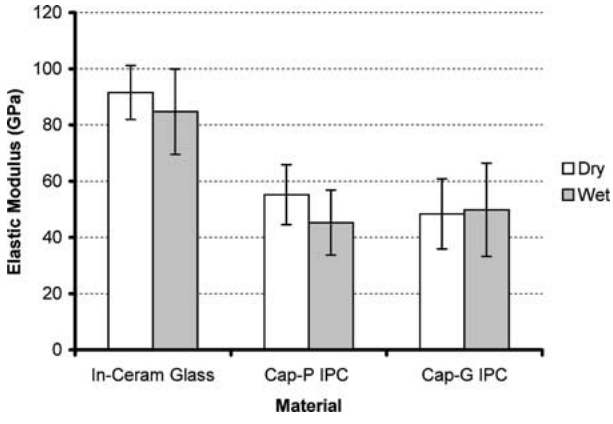

Figure 4 Histogram showing the mean elastic modulus (GPa) calculated from measurements of the linear elastic portion of the stress-strain curve for each specimen tested in air and in water. Vertical error bars represent the standard deviation for each sample and in all cases, n = 20.

of In-Ceram glass specimens is decreased by approximately 28% when tested in a moist environment relative to the strength of samples tested in air. A similar reduction in measured strength (32%) occurred in the wet Cap-G IPC. The Captek-P/In-Ceram glass IPC displays higher strength when tested wet (146.29 ± 24.30 MPa compared with 135.25 ± 29.75 MPa when tested dry) however this difference was shown not to be significant according to a One Way Analysis of Variance (ANOVA) with post hoc Tukey test. The same test revealed that there was no significant difference between the dry strengths of all the materials in the study. Additionally there was no significant difference between the wet strengths of the Cap-G IPC and In-Ceram glass samples, although they both displayed significantly lower strengths than the Cap-P IPC tested wet.

Mean elastic moduli are presented for each sample group in Fig. 4. No significant difference was identified between the elastic modulus of the Cap-P and Cap-G IPCs. Both IPC systems displayed significantly reduced elastic moduli compared with the single-phase In-Ceram glass control specimens. However the test environment did not significantly influence the elastic modulus of any of the materials examined in the current study.

Toughness can be deduced from the mean values for the area under the stress-strain curve for each sample

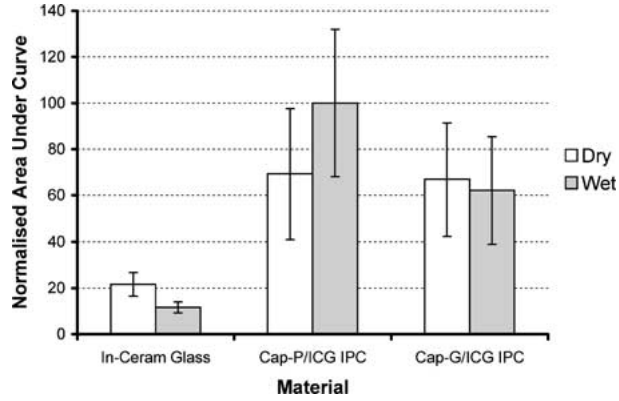

Figure 5 Histogram showing normalised mean values of area under the stress-strain curve for each specimen. Vertical error bars show the standard deviation.

in Fig. 5. One Way ANOVA with post hoc Tukey tests were again employed to statistically analyse the data and showed that both IPC systems absorbed significantly more energy prior to failure than the glass system alone. No significant difference was observed between the data for both the dry and wet In-Ceram glass specimens or between the dry and wet Cap-G IPC specimens. However the area under curve was shown to increase significantly when the Cap-P IPC was tested in a moist environment as opposed to testing dry.

SEM analysis of polished cross-sections revealed that the thermal treatment used to remove the organic binder from the as supplied Cap-P and Cap-G materials resulted in the formation of porous bodies as shown in Figs 1 and 2 respectively. The interleaved arrangement of particles in the Cap-P ribbon prior to removal of the organic binder is expressed in the de-waxed preform, and particle fusion at points of contact results in the formation of a convoluted network of interconnected porosity. The predominately spherical, loosely packed particles in the Cap-G system partially sinter during de-waxing to create a more open network of porosity with reduced interconnectivity compared to the Cap-P preform. Image analysis revealed the pore volume in the Cap-P and Cap-G preforms to be $40.2 \pm 3.3\%$ and $21.8 \pm 7.9\%$ respectively. The firing schedules used to infiltrate glass into each preform result in further microstructural modification as shown in Figs 6 and 7, which depict Cap-P/In-Ceram glass and Cap-G/In-Ceram glass IPCs respectively. Despite the obvious microstructural differences it was calculated that there was no significant difference between the relative constituent phase volumes in both specimens, the Captek-P IPC containing $29.1 \pm 2.9\%$ glass (originally pore volume), the Captek-G IPC containing $32.4 \pm 6.5\%$ glass.

The deformation characteristics of the materials under test are shown in Fig. 8, these plots having been selected as they exhibit closest stress at failure to the mean from their data set. In-Ceram glass shows perfectly linear ($R^2 = 1$) elastic behaviour until the failure stress is reached. Failure is by sudden and catastrophic initiation and propagation of a crack through the specimen; classically brittle behaviour. The Cap-G/ICG composite shows a linear elastic region between 0 to 0.10% strain ($R^2 = 0.99$) however when strain $\geq$0.10%

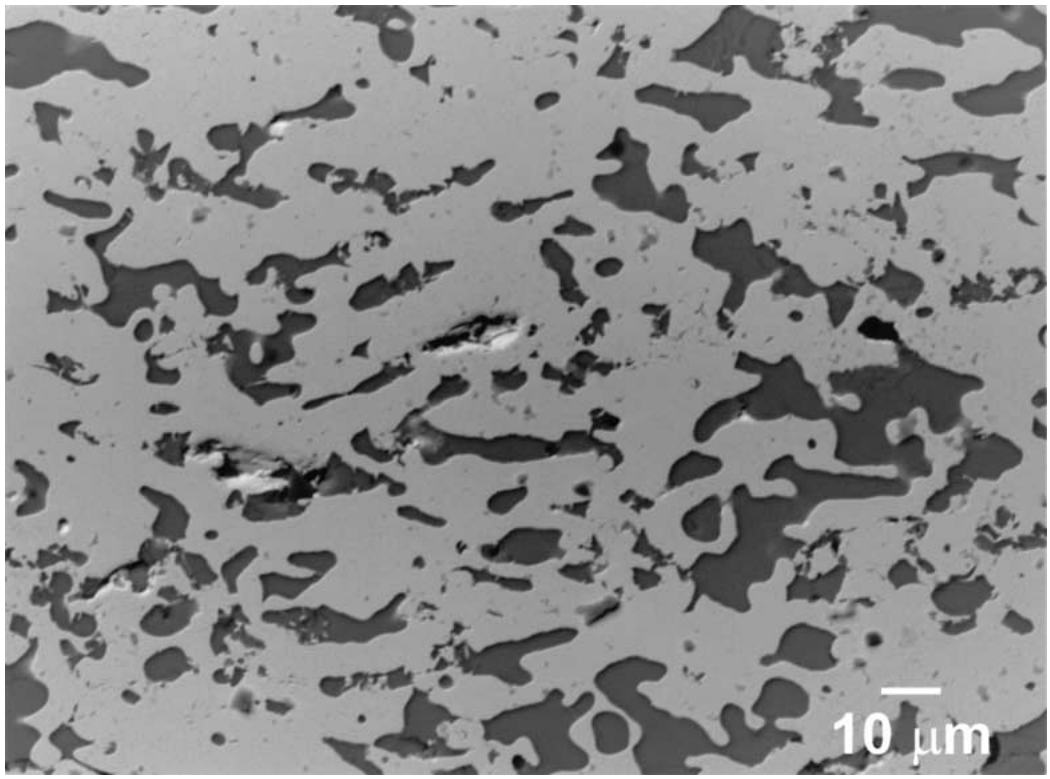

Figure 6 Backscattered SEM micrograph at ×750 magnification of a longitudinal cross section through the glass-infiltrated Cap-P IPC. The metallic phase is the lighter of the two principal tones of the image, whilst the glass is darker.

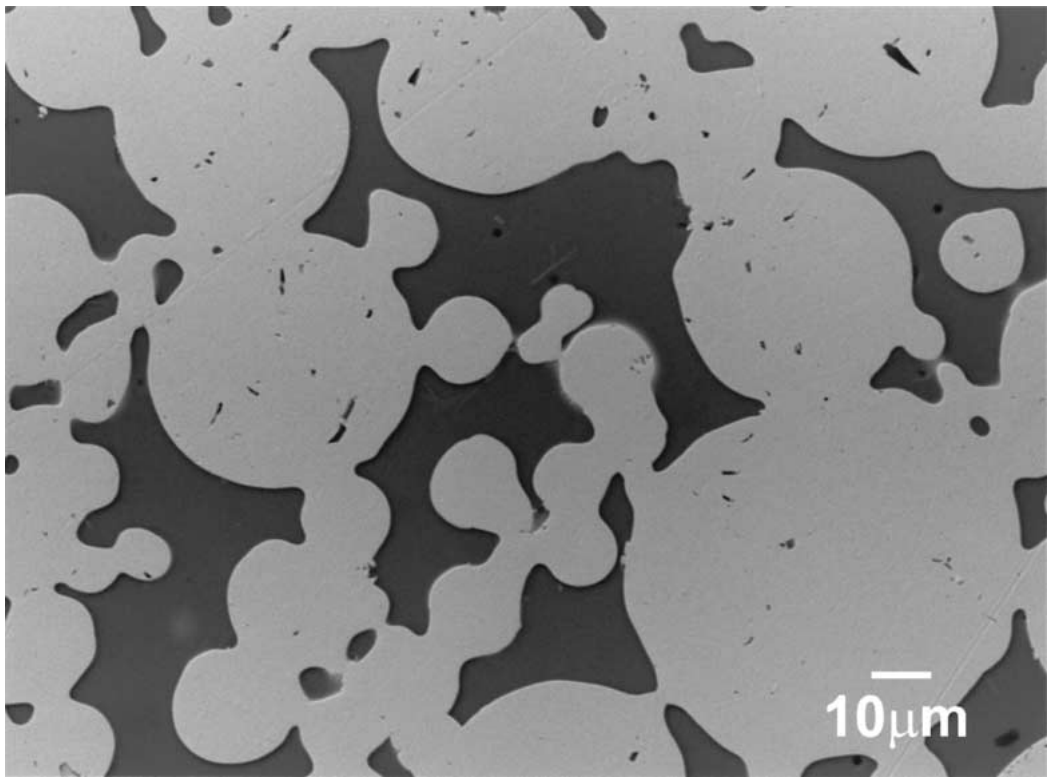

Figure 7 Backscattered SEM micrograph at ×750 magnification of a longitudinal cross section through the glass-infiltrated Cap-G IPC. The metallic phase is the lighter of the two principal tones of the image, whilst the glass is darker.

the gradient of the line begins to decline producing a smooth curve. The material continues to deform until the stresses present are sufficient to cause fast fracture. The Cap-P IPC behaves similarly although with the sample shown the linear elastic region occurs between 0.75–1.6% strain after what appears to be a bedding-in period, and the strain to failure is slightly increased.

4. Discussion

The mean 3-point flexural strengths of each material tested dry are not significantly different, suggesting that an interpenetrating metal phase serves primarily to adjust the deformation and failure behaviour (see Fig. 8) of the In-Ceram glass. The 28% reduction in strength of the In-Ceram glass after wet storage is consistent

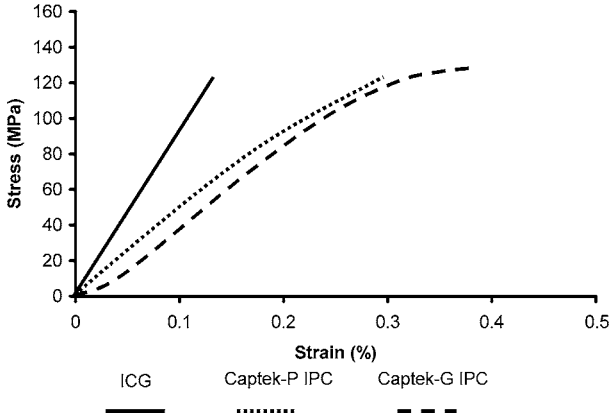

Figure 8 Typical stress-strain profiles for each material tested in 3-point bend.

with the theory that a moist environment can contribute to the sub-critical advancement of a crack in an unstressed ceramic body as a consequence of hydration of metal-oxygen bonds at the crack tip [20]. Significantly this is also identical to data produced by Hornberger [21] for the complete In-Ceram system in which a 28% strength reduction was observed after immersion in water for 1 week (170 hrs).

Statistically significant differences were observed in strength between the IPC materials tested wet, the Cap-G IPC suffering a near identical reduction in flexural strength to the glass control when exposed to moisture. However the Cap-P IPC shows no measurable reduction in strength, indicating that the presence of an interpenetrating metal phase does not automatically confer resistance to environmentally assisted slow crack growth. Considered in conjunction with the Hornberger data [21], this suggests that in addition to the material from which the reinforcing phase is made, its microstructural arrangement (in terms of particle morphology) and degree of interconnectivity must play a significant role in the way crack propagation takes place within IPC systems. A more comprehensive understanding of crack propagation could be achieved through a detailed fracture mechanics study, but to be effective this would demand the production of statistically reproducible microstructures and larger samples to facilitate resolution to the experimental challenge of producing notched test samples. Such an approach was thus outside the scope of the current investigation due to the small size of test sample necessitated by material cost and manufacturing constraints.

The microstructures of both IPCs (see Figs 6 and 7) differ principally in the fact that the number of interconnections between metal particles is greater in the Cap-P substructure than it is in the Cap-G. The latter contains larger regions of uninterrupted glass through which a crack may propagate to weaken the composite system. The number of interconnections between component particles is related to their overall morphology. The interleaved arrangement of flake-shaped particles of the Cap-P provides more interparticle contact points than the loosely packed, spherical particles of the Cap-G. For a crack to propagate through the bulk of a Cap-P IPC specimen it must transect metal particles, as shown in Fig. 9 (p), or fused regions between metal particles (approximately similar in thickness to the particle bulk). Given that in the Cap-P IPC system, the reinforcing phase is relatively uniformly distributed with respect to the material bulk, the crack stopping potential of this system is expected to deviate little according to the location of the crack within the specimen.

By comparison the spherical morphology of the Cap-G particles creates interparticle necks as a result

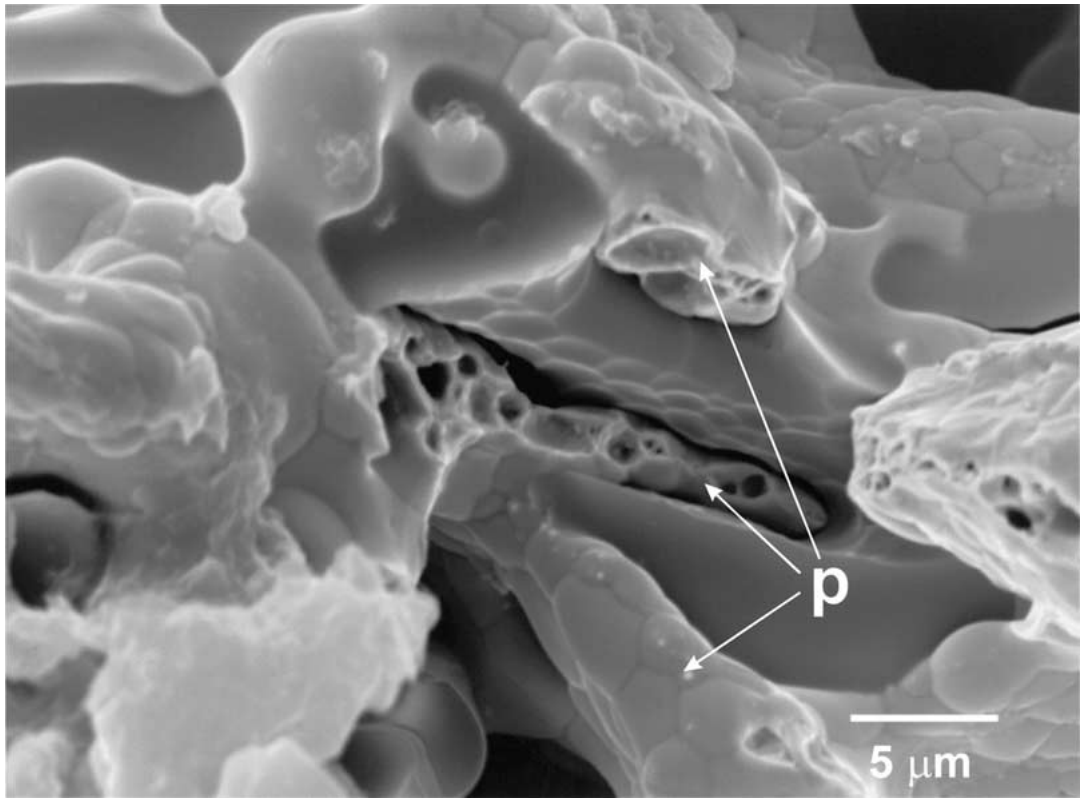

Figure 9 Secondary electron SEM image at ×3,500 magnification of a fracture surface formed in the Cap-P IPC.

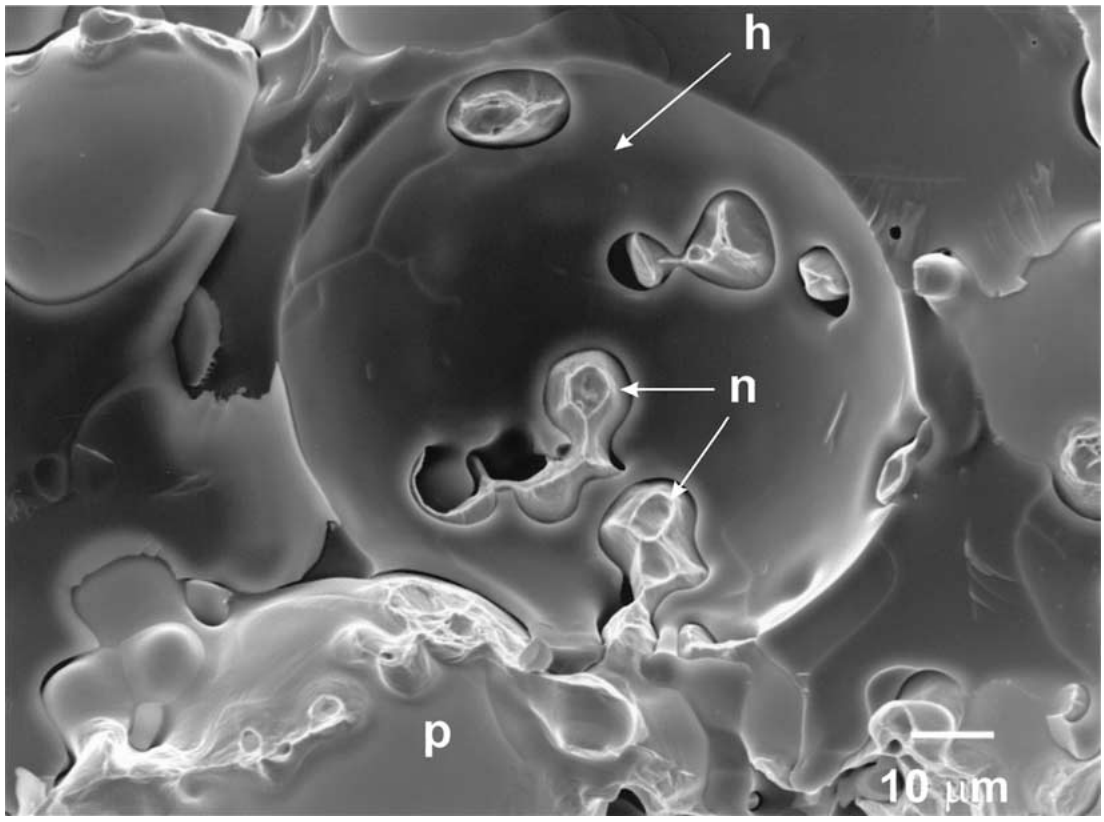

Figure 10 SEM micrograph at ×1,000 magnification of a fracture facet in a Cap-G IPC specimen.

of partial sintering, which due to their reduced diameter relative to the particle bulk represent areas of highest stress within the metal substructure when loaded. Furthermore the larger volumes of uninterrupted glass make it possible that relatively high crack velocities will be attained prior to arrival of the crack at a metal-glass interface. Upon arrival at a spherical particle the crack is more likely to be deflected (as opposed to proceeding through the particle bulk) and will subsequently travel along the path of least resistance in order to propagate, in this case around the perimeter of the sphere along the metal-glass interface. Although well formed in terms of close adaption of the glass to the surface of the metal phase, there is little evidence to suggest that chemical bonding has occurred at the interfacial region and therefore little resistance to circumvention of the particle by the crack front is to be expected. Advancing cracks will encounter and attempt to propagate past interparticle necks, which subsequently become bridging ligaments and exert a closure stress on the two fracture facets in the brittle material. An example of such a phenomenon is shown in Figs 10 and 11, which depict a typical fracture surface from the Cap-G IPC. The hemispherical concavity (h) at the centre of Fig. 10 is the result of spherical particle detachment, the particle concerned comprising part of the other specimen fragment created as a result of final fracture. A similar particle that remained with the portion of sample in view is shown (p) standing proud of the fracture through the brittle glass phase. Visible toward the apex of the concavity are several isolated portions of gold (n). These are interparticle necks that have failed after extensive plastic deformation producing the characteristic cup-and-cone fracture facet (shown at high magnification in Fig. 11) associated with the ductile failure of metals in tension. Although not expressed to the same extent in the Cap-P IPC, the evidence of brittle failure of the glass combined with plastic deformation prior to ductile failure of the metal on the fracture facets for the Cap-G system is consistent with data from many other studies. Images of the fracture surfaces of AlN/Al [14], Al_2O_3/Al [4, 22] and Al_2O_3/Al(Si) [23] IPCs have been published which morphologically bear a very strong resemblance to the images presented here. The theory of ductile ligament formation followed by plastic deformation and ductile failure in the wake of a crack advancing through the brittle phase appears to be accepted throughout the literature.

The dramatic reduction (approximately 47%) in measured elastic modulus when an interpenetrating metal is introduced to the glass is an interesting feature, although difficult to analyse in view of the fact that corresponding data was not produced for the metallic components alone. The severity of the reduction forces consideration of possible explanations, particularly given that the measured modulus of the IPC was recorded as being lower than that of elemental gold; a particularly ductile metal and that which comprised part of the Cap-G IPC system. The presence of unfilled porosity within the test specimens was not fully verified and could account for some of the decrease, given that pores must contain air, which has an elastic modulus of zero. The use of non-standard specimen dimensions, mandated by the need for material economy and difficulties associated with sample manufacture could also account for discrepancies between measurements

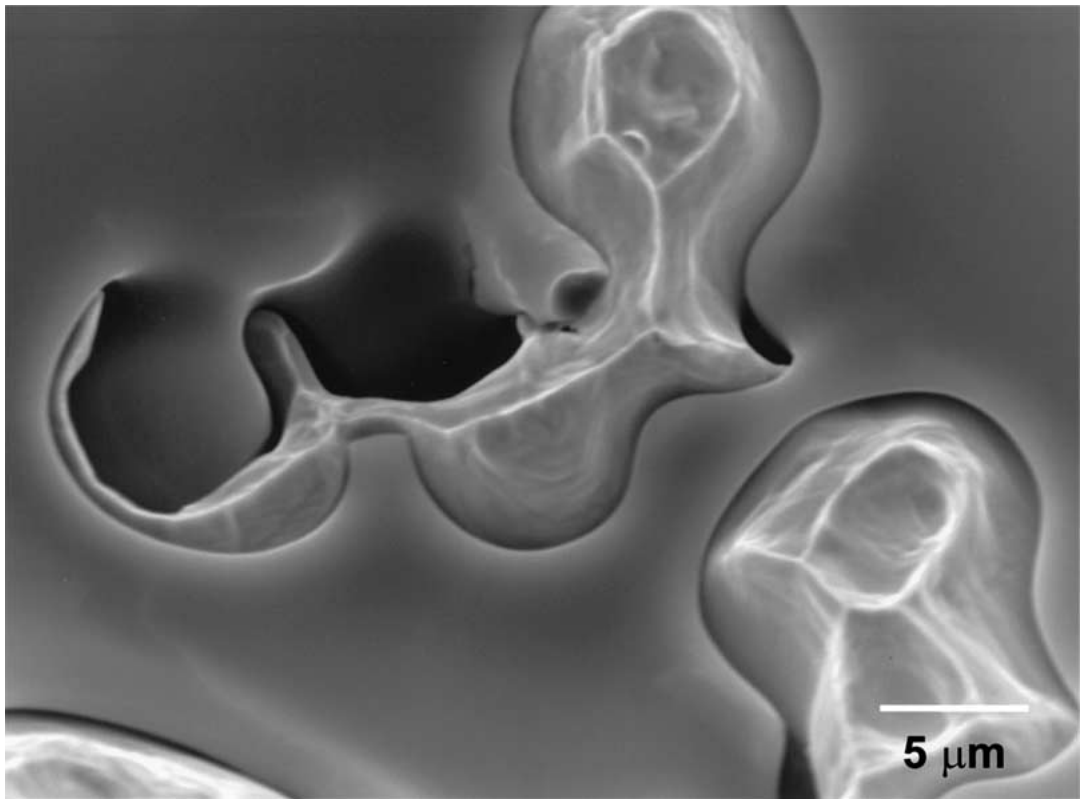

Figure 11 Higher magnification (×3,500) secondary electron SEM image showing the interparticle necks identified as n in Fig. 10.

on these IPCs and other systems. However methods and specimen sizes were constant throughout all procedures so data produced by the glass control and the Cap-G and Cap-P IPCs for comparative purposes should remain valid.

It is apparent that many factors govern the expression of mechanical properties of an IPC system including volume fraction of constituent phases, morphological arrangement of those phases and the properties of the individual constituent materials themselves. For example, the spatial arrangement of "particles" in a preform containing interpenetrating porosity has been shown to exert influence over environmental effects on strength whilst having, as the results of this study suggest, little if any influence upon dry strength. Generally speaking there exists a serious lack of clarity regarding which factors control which aspects of the expressed mechanical behaviour of IPC systems, notwithstanding the fact that educated deductions hint at certain areas of dominance. This, in combination with the fact that most (if not all) IPCs manufactured to date possess random microstructural architectures, mandates that some extremely complex mathematics are required to allow any sort of predictive modelling of IPC behaviour. A key requirement within the field of IPC research must therefore be to establish a set of rules regarding the type of behaviour that can be expected for different material combinations, at different volume fractions, with different morphological arrangements. The ease with which such rules might be formulated would depend to a considerable extent on the availability, or reproducibility of IPCs having identical microstructures. Such materials would allow the construction of an experiment, perhaps incorporating a factorial analysis, to assess each performance-affecting factor against all the others in an ordered, methodical manner, whilst avoiding the need for exceptionally large numbers of specimens as would be the case with a classical experiment design.

5. Conclusions

The manufacture of glass-metal IPC systems is possible through the infiltration of molten glass into a porous metallic network through capillary forces. Materials produced this way show a significant reduction in measured elastic modulus relative to the base glass. Although volume fraction and the network morphology clearly affect the mechanical properties of such systems the relevance of each parameter to the bulk characteristics of the composite are yet to be fully understood. The tri-dimensionally co-continuous nature of the reinforcement in IPC systems offers potential resistance to environmentally assisted crack growth, although this is not a default feature of such systems and appears again to be morphologically dependent. IPCs represent a highly interesting class of material, however their development to a point at which commercial implementation can be seriously considered on a regular basis is at present hindered by a lack of understanding of the interaction between the many factors present in these systems. The production of IPC systems with completely reproducible microstructures (not subject to random particle arrangements or reaction nucleation positions) will allow more focused work to proceed. This will lead to the depth of understanding necessary to allow predictive rules to be established regarding IPC behaviour and then take full advantage of the property-tailoring opportunities which IPCs present.

References

1. S. D. CAMPBELL, L. B. PELLETIER, R. L. POBER and R. A. GIORDANO, *J. Prosthet. Dent*. **74** (1995) 332.
2. I. SHOHER and A. E. WHITEMAN, US Patent no 5,593,305 (1997).
3. R. M. DE SOUZA, H. N. YOSHIMURA, C. XAVIER and H. GOLDENSTEIN, *Key Eng. Mat.* **127–131** (1997) 439.
4. M. C. BRESLIN, J. RINGNALDA, L. XU, M. FULLER, J. SEEGER, G. S. DAEHN, T. OTANI and H. L. FRASER, *Mat. Sci. Eng.* A **195** (1995) 113.
5. R. E. LOEHMAN, K. EWSUK and A. P. TOMSIA, *J. Amer. Ceram. Soc.* **79**(1) (1996) 27.
6. W. ZHOU, W. HU and D. ZHANG, *Scripta Mater.* **39** (1998) 1743.
7. H. J. FENG and J. J. MOORE, *Met. Mat. Trans.* B. **26B** (1995) 265.
8. X. M. YUE, G. J. ZHANG and Y. M. WANG, *J. Euro. Ceram. Soc.* **19** (1999) 293.
9. T. KLASSEN, R. GUNTHER, B. DICKAU, F. GARTNER, A. BARTELS, R. BORMANN and H. MECKING, *J. Amer. Ceram. Soc.* **81**(9) (1988) 2504.
10. J. W. CAHN and R. J. CHARLES, *Phys. Chem. Glasses* **6**(5) (1965) 181.
11. L. D. WEGNER and L. J. GIBSON, *Int. J. Mech. Sci.* **42** (2000) 943.
12. *Idem*., *ibid*. **42** (2000) 925.
13. D. P. SKINNER, R. E. NEWNHAM and L. E. CROSS, *Mat. Res. Bull.* **13** (1978) 599.
14. C. TOY and W. D. SCOTT, *J. Amer. Ceram. Soc.* **73**(1) (1990) 97.
15. J. RODEL, H. PRIELIPP, N. CLAUSSEN, M. STERNITZKE, K. B. ALEXANDER, P. F. BECHER and J. H. SCHNIEBEL, *Scripta Metall. et Mater.* **33**(5) (1995) 843.
16. S. N. WHITE, A. A. CAPUTO, F. M. A. VIDJAK and R. R. SEGHI, *Dent. Mater.* **10** (1994) 52.
17. H. CLAUS, *Quintessenz Zahntech.* **16** (1990) 35.
18. H. LEVY, *Prosthèse Dentaire.* **44/45** (1990) 1.
19. R. A. GIORDANO, L. PELLETIER, S. CAMPBELL and R. POBER, *J. Prosthet. Dent.* **73**(5) (1995) 411.
20. J. E. RITTER, *Dent. Mater.* **11** (1995) 142.
21. H. HORNBERGER, PhD Thesis, The University of Birmingham (1995).
22. B. D. FLINN, M. RUHLE and A. G. EVANS, *Acta. Metall.* **37**(11) (1989) 3001.
23. K. G. EWSUK, S. J. GLASS, E. LOEHMAN, A. P. TOMSIA and W. G. FARENHOLTZ, *Met. & Mat. Trans* A. **27A** (1996) 2122.

Received 4 April 2001
and accepted 7 February 2002